Supporting Information

Highly Selective Detection of Trinitrophenol by Luminescent Functionalized Reduced Graphene Oxide through FRET mechanism

Diptiman Dinda, Abhisek Gupta, Bikash Kumar Shaw, Suparna Sadhu and Shyamal Kumar Saha*

Department of Materials Science
Indian Association for the Cultivation of Science, Jadavpur
Kolkata 700032

*Email of corresponding author: cnssks@iacs.res.in

1. **Nitroexplosive Materials:**

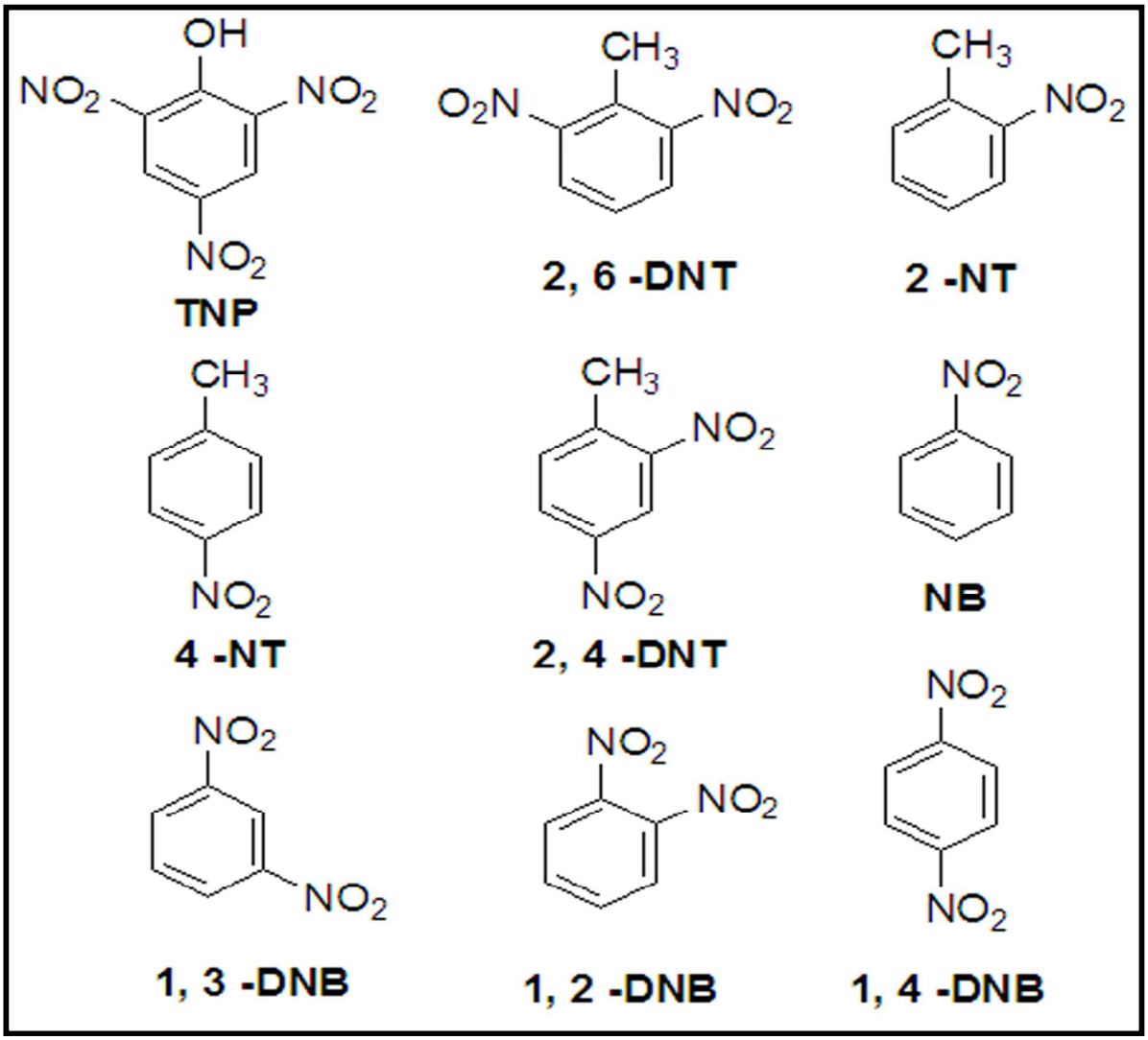

Scheme S1: Structures of all the nitroexplosives used in this experiment

2. Chemical Synthesis of DAP-RGO:

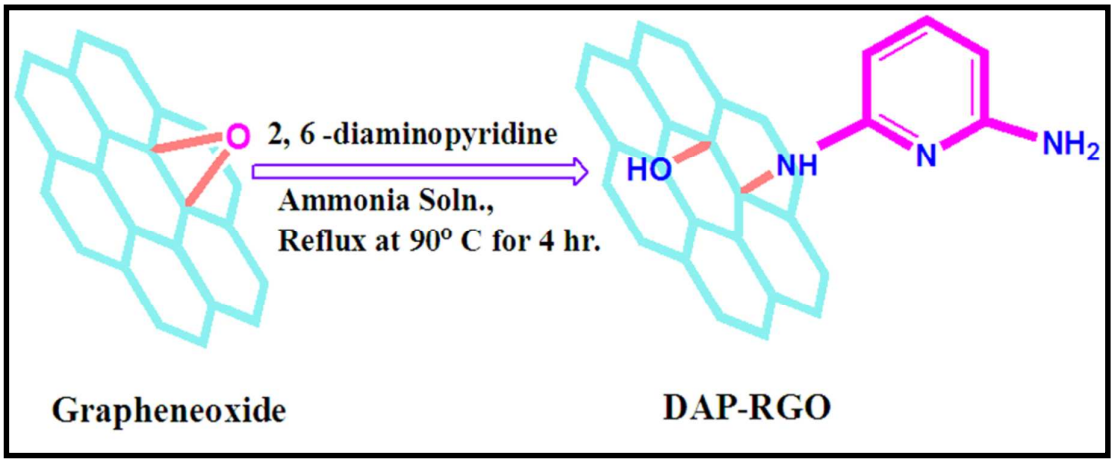

Scheme S2 Schematic diagram for the synthesis of DAP-RGO through functionalization of graphene oxide

3. General characterizations:

The obtained DAP-RGO material has been charecterized using FTIR, XPS, TGA, UV-Vis and XRD measurements. Detailed charecterization of this material is reported in our previous work.[1]

Amine group of 2,6-diaminopyridine attacks the epoxy groups at the GO surface forming this compound DAP-RGO via S_N2 reaction. The absance of epoxy peaks (1070 cm^{-1}) and appearance of N-H peaks (3388 for 1^0 amine and 3336 cm^{-1} for 2^0 amine) in the FTIR spectra in our prepared material confirms the functionalization of graphene oxide. From XPS measurement, two additional peaks for C-N, C=N (285.6 and 286.2 eV) and much lowering intensity of C-O peak compare to GO are observed in the deconvoluted C_{1S} spectra of DAP-RGO material which confirm functionalization of GO by amine groups. In TGA analysis, much sharper weight loss between 130 ^{0} C to 300 ^{0} C and 34% residual weight at 800 ^{0} C compare to GO also confirms the conversion of GO to more stable DAP-RGO through

functionalization. The red shifted π-π* transition peak (from 228 to 245 nm) and a intensed n-π* transition peak (309 nm) compare to GO in UV-Vis spectra strongly suggest that GO has been functionalized by 2,6-diaminopyridine at the epoxy sites to form more stable DAP-RGO material. We have also carried out XRD measurements on both virgin GO sample and functionalized DAP-RGO sample. A broad intense peak at ~12^0 is observed for virgin sample which corresponds to its GO phase. However, the DAP-RGO sample shows a broad graphene peak at ~25^0 at the cost of very small GO peak. No peak is observed at lower angle (<10^0) which should have appeared as a result of increasing interlayer separation due to attachment of both amine ends of DAP with two different GO sheets.[2] This result confirms that there no aggregation of GO sheets during functionalization.

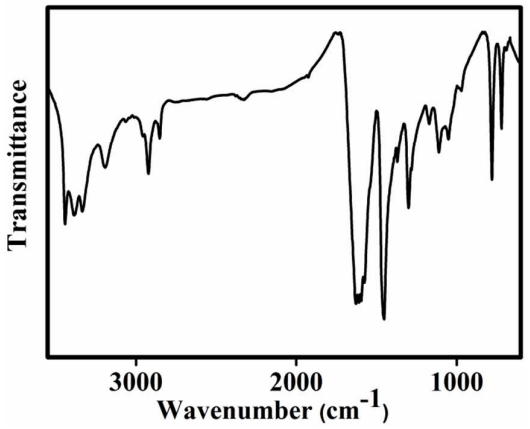

Fig. S1 FTIR spectra of DAP-RGO composite

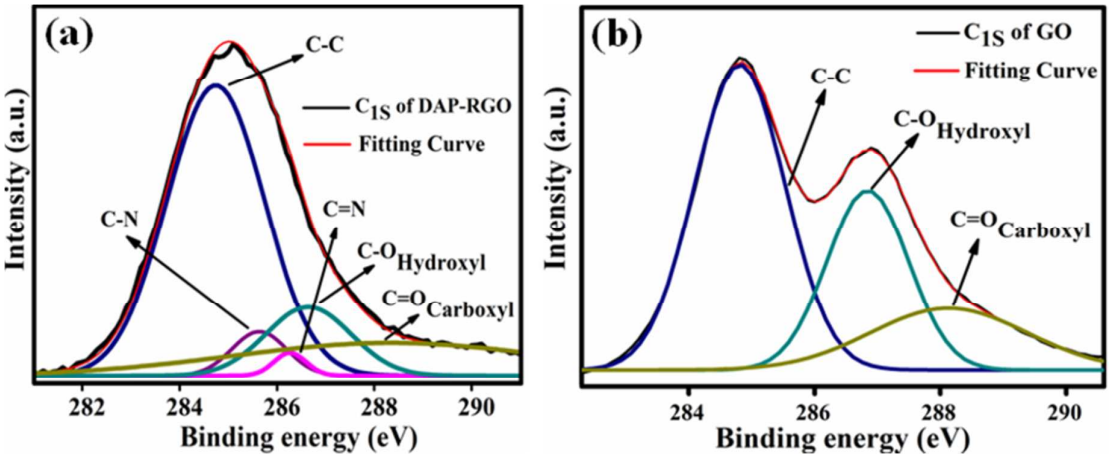

Fig. S2 (a) Deconvoluted C_{1S} XPS spectra of DAP-RGO composite and (b) GO

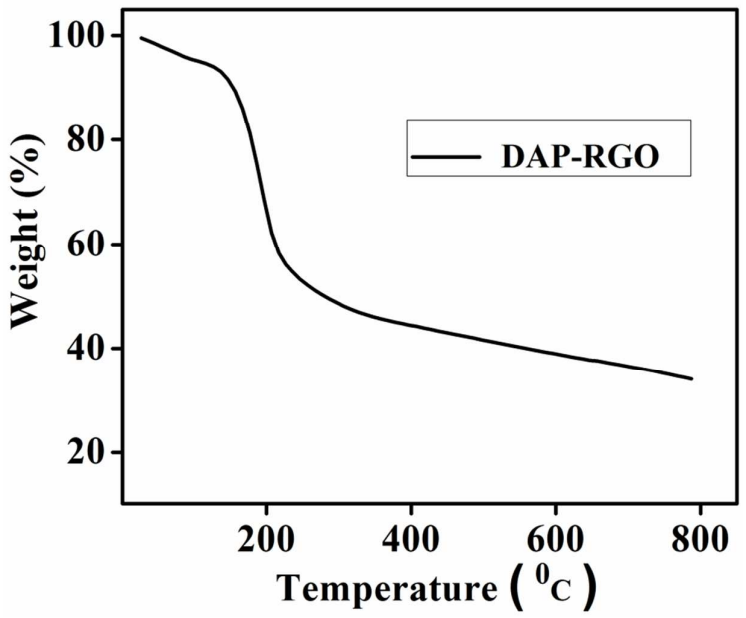

Fig. S3 TGA curve of DAP-RGO composite

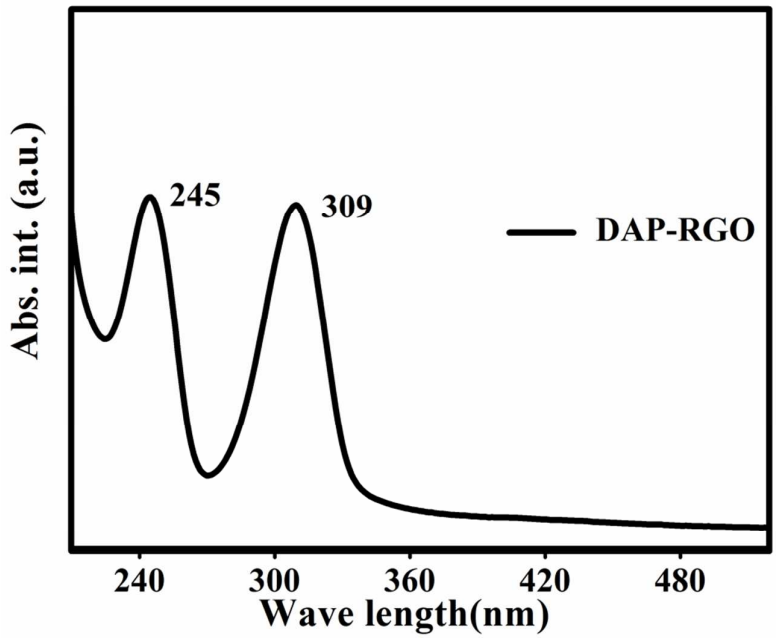

Fig. S4 UV-Vis spectra of DAP-RGO composite

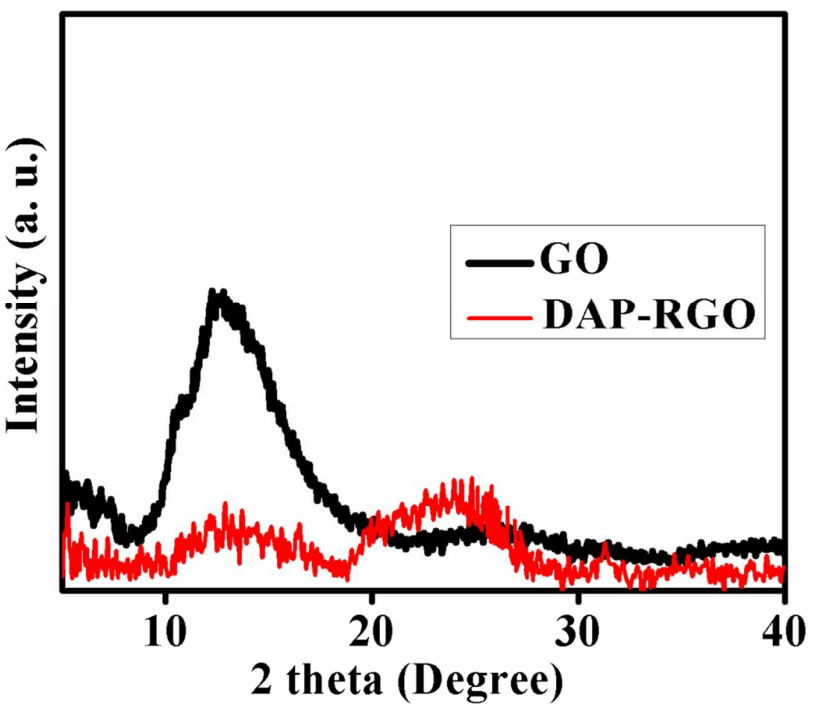

Fig. S5 XRD image of GO and DAP-RGO

4. Quantum Yield (QY) measurement:

Quinine Sulfate in 0.1M H2SO4 (Φr (QY) = 0.54) is chosen as reference.[3] Relative fluorescence quantum yield of the sample DAP-RGO and GO are calculated according to the following expression (i)

$$\Phi s = (Is/Ir) \times (Ar/As) \times (\eta s2/\eta r2) \times \Phi r \qquad (i)$$

Where the subscripts r and s refer to the reference and the sample respectively, Φ is the fluorescence quantum yield, I is the measured integrated fluorescence emission intensity, A is the optical density and η is the refractive index of the solvents.

Our synthesized DAP-RGO gives 18.67 % QY whereas, GO shows only 0.02 %. This result strongly reveals that non-emissive GO has been converted to highly luminescent DAP-RGO through functionalization by DAP molecules at the epoxy sites of GO sheets.

5. Exication dependant photoluminescence Study:

Our prepared material also exhibits excitation dependent PL behaviour. From Fig. S3, it is seen that when the excitation wave length changes from 300 nm to 450 nm, the emission maxima shift from 368 nm to 523 nm accompanied with the gradual change in emission intensity at a fixed pH value of 4. This result suggests the existence of both the heterogeneous electronic structures attribute to the multi-distribution of sp^2 cluster sizes in DAP-RGO material during functionalization.[4]

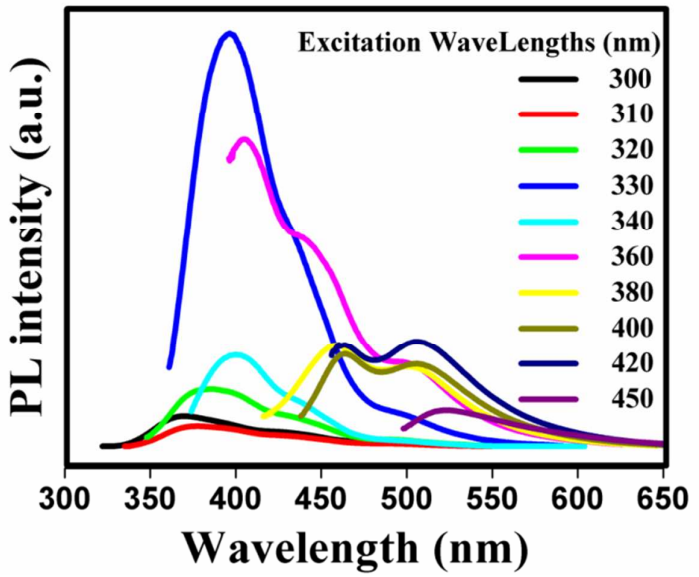

Figure S6 Excitation dependent PL of DAP-RGO

6. Fluorescence quenching titration experiments:

We have also studied the fluorescence quenching experiments for different nitro explosives but these shows very weak PL quenching to DAP-RGO compare to TNP. The quenching efficiency plots are given below for those nitro compounds.

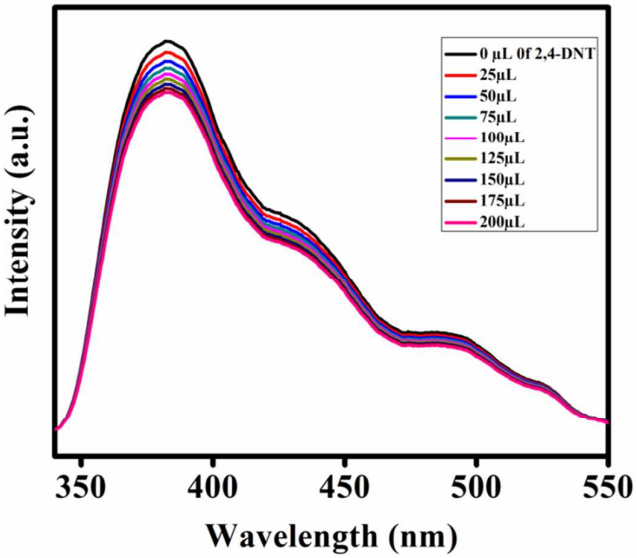

Figure S7 : PL quenching upon increamental addition of 1mM 2, 4-DNT solution at buffer 7.

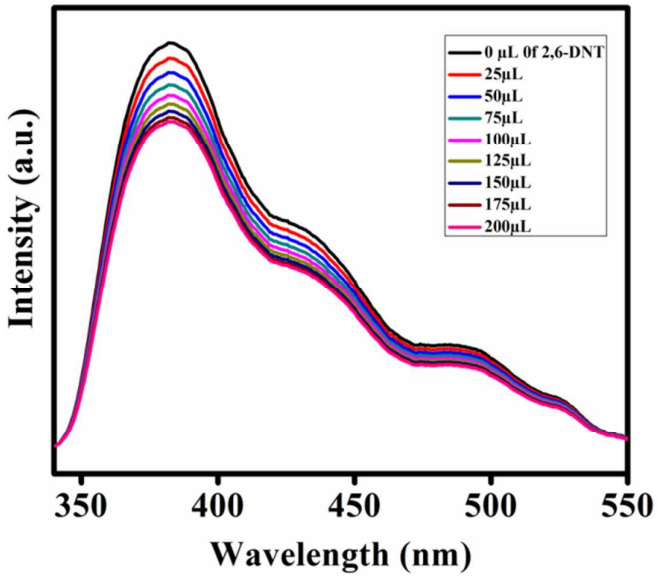

Figure S8 : PL quenching on addition of 1mM 2, 6 -DNT solution at buffer 7.

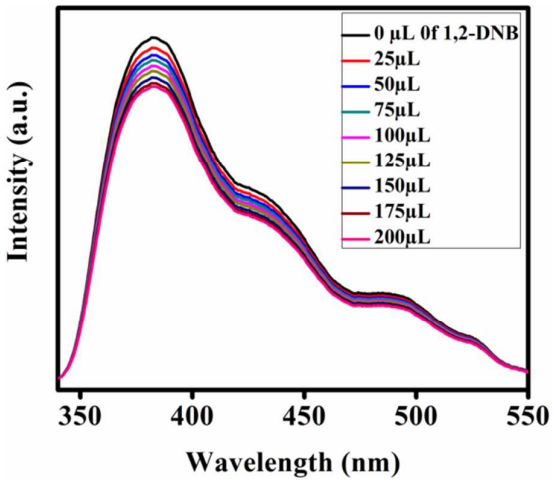

Figure S9 : PL quenching with addition of 1mM 1,2 -DNB solution at buffer 7.

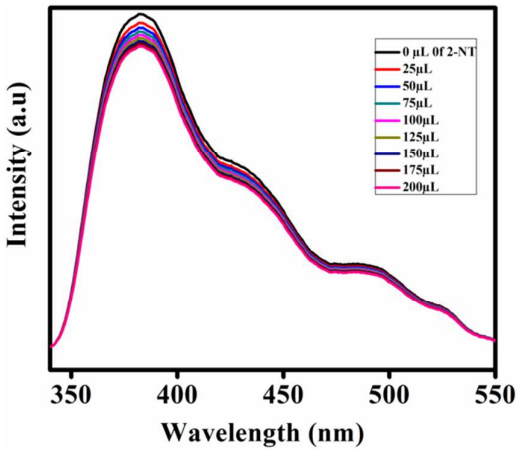

Figure S10 : PL quenching with addition of 1mM 2- NT solution at buffer 7.

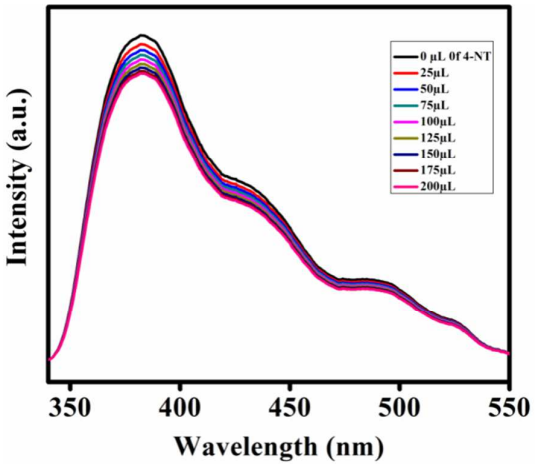

Figure S11 : Fluorescence quenching adding 1mM 4 – NT solution at buffer 7.

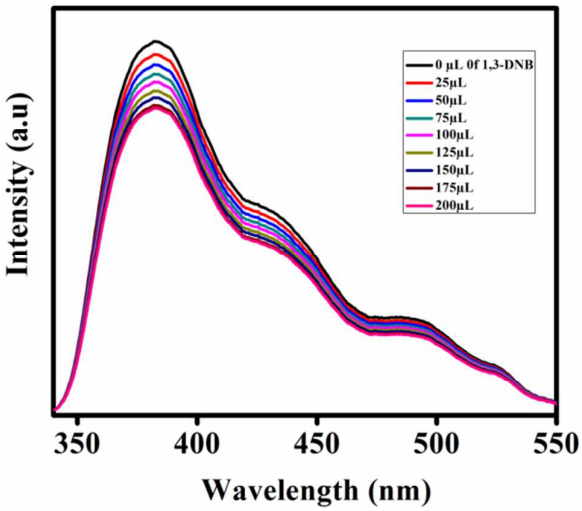

Figure S12 : Fluorescence quenching by adding 1mM 1, 3-DNB solution at buffer 7.

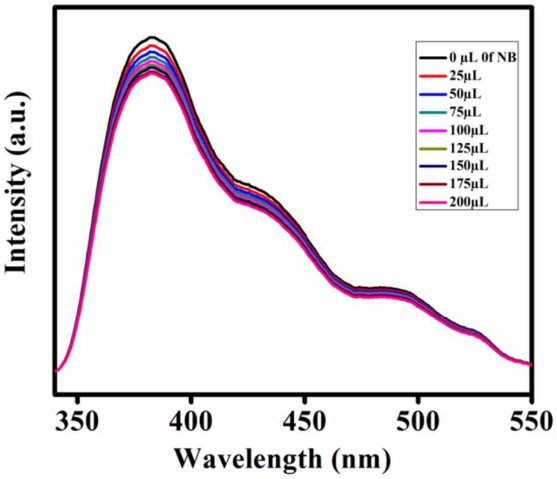

Fig. S13 : PL quenching upon increamental addition of 1mM NB solution at buffer 7.

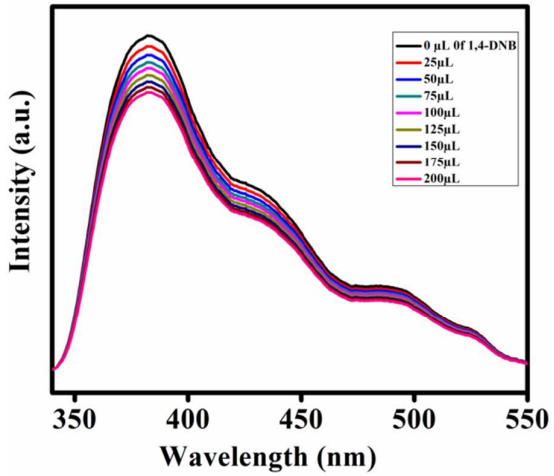

Figure S14 : Fluorescence quenching for 1,4-DNB upon addition of 1mM solution.

7. Calculation of Detection Limit for TNP:

The detection limit for TNP is calculated from fluorescence quenching experiment of DAP-RGO with addition of TNP. The intercept (log[TNP]) to X-axis is obtained by linear plot of the $(I_{max}\text{-}I)/(I_{max}\text{-}I_{min})$ vs. log[TNP], where I_{max}, I and I_{min} are the initial fluorescence intensity, intensity at different TNP concentration and intensity at saturation point respectively. Detection limit is calculated using formula, $([TNP] \times MW_{TNP})/1000)$ and multiplying this with factor10^9, we get the detection limit value in ppb.[5] Here, MW_{TNP} is the molecular weight

of TNP. The calculated detection limits for TNP is 125 ppb using our prepared DAP-RGO as sensor.

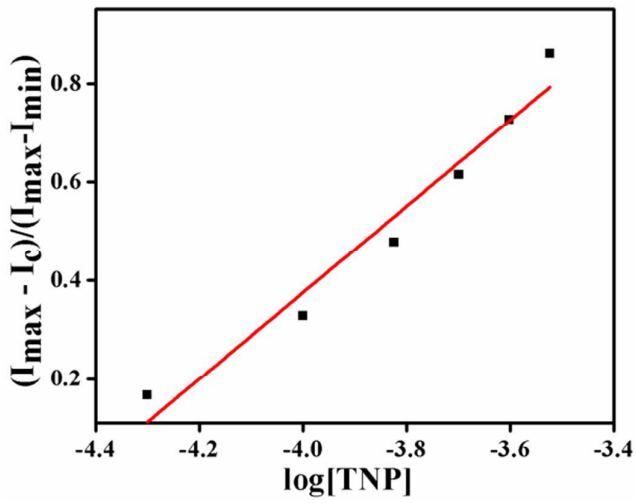

Fig S 15: Detection limit of TNP by DAP-RGO composite

8. Fluorescence decay measurements:

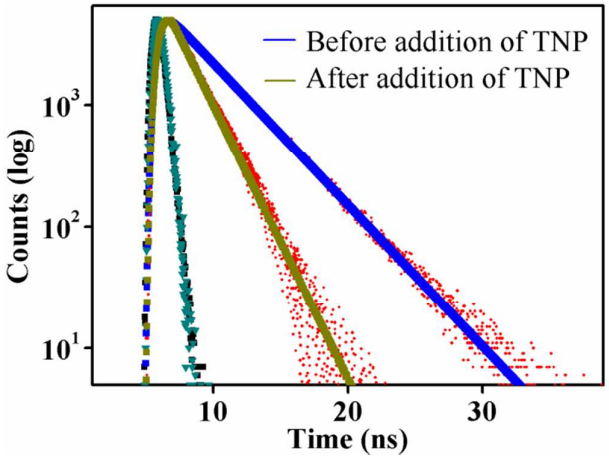

Fig S16: Time-resolved fluorescence decay curve of DAP-RGO composite

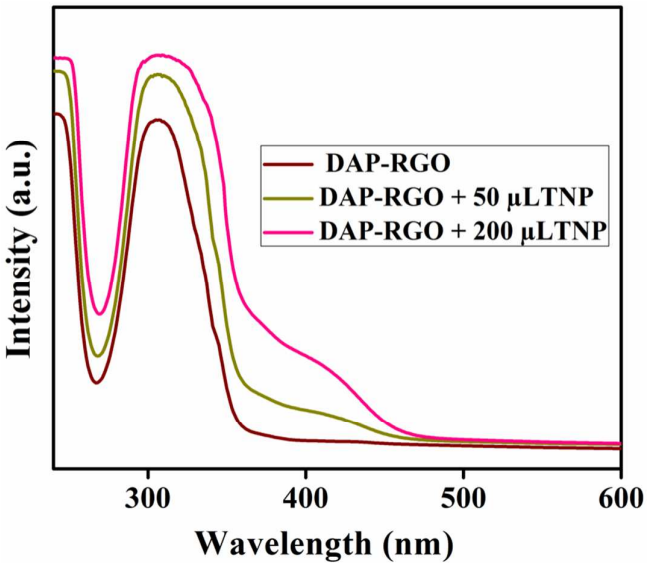

Figure S17 Change in Absorption spectra of DAP-RGO upon addition of TNP solution.

From Fig. S18, it is observed that a new absorption band is observed at 410 nm and its intensity also increases with gradual addition of TNP solution. From this, it may be conclude that a new chrage transfer complex is formed between them as a result of proton transfer from TNP to our prepared material DAP-RGO.

9. DFT optimized structure for 2, 6-DNT and DAP-RGO:

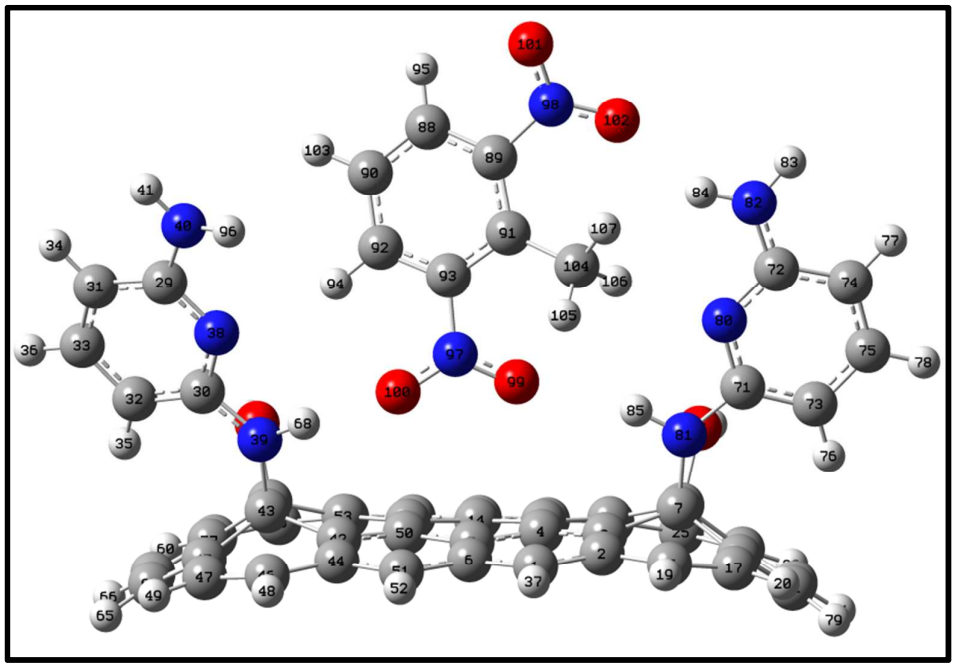

Fig. S18: DFT optimized structure of 2, 6-DNT and DAP-RGO

10. Fluorescence quenching for different nitro-phenols:

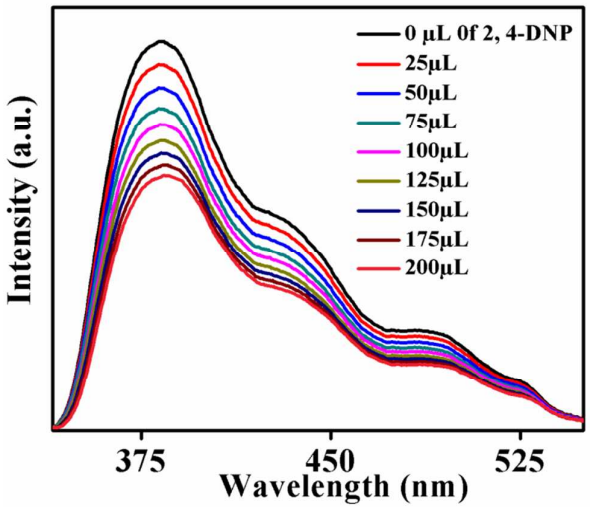

Fig. S19 : PL quenching upon increamental addition of 1mM 2, 4-DNP solution at buffer 7.

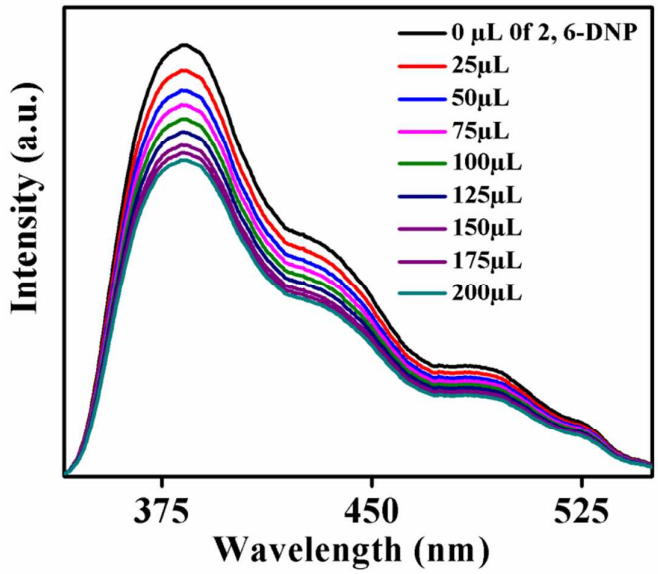

Fig. S20 : PL quenching upon increamental addition of 1mM 2, 6-DNP solution at buffer 7.

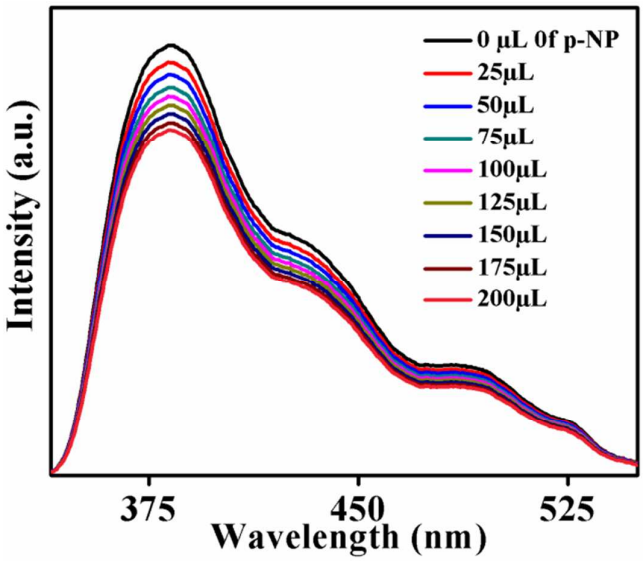

Fig. S21 : PL quenching upon increamental addition of 1mM p-NP solution at buffer 7.

Table S1 : Comparision of quenching constants (K_{S-V}) in literature :

Materials	K_{SV} values (M^{-1})	Referances
Pentacenequinone derivative	1.55×10^{4}	Appl. Mater. Interfaces 2013, 5, 672−679
Tetraphenylethelene nanosphere	3.0×10^{4}	Chem. Eur. J. 2013, 19, 1 – 8
Cd based MOF	3.5×10^{4}	Angew. Chem. Int. Ed. 2013, 52, 2881-2885
Tris imidazolium salt	3.8×10^{4}	J. Org. Chem. 2013, 78, 1306−1310
p-phenylenevinylene probe	5.51×10^{4}	Appl. Mater. Interfaces 2013, 5, 8394−8400
2, 6-DAP functionalized Graphene oxide	1.322×10^{5}	**Present Work**

Table S2 : HOMO – LUMO energies for different nitro aromatic explosives and DAP-RGO composite as calculated by B3LYP/6-31G* DFT model :

Explosives	HOMO (eV)	LUMO (eV)	Bandgap (eV)
TNP	-8.829	-4.833	3.996
2,4 - DNT	-8.532	-3.834	4.698
2 – NT	-7.34	-2.75	4.59
4 – NT	-7.695	-3.186	4.509
1,3 –DNB	-8.856	-4.023	4.833
NB	-7.938	-3.321	4.617
1,4- DNB	-8.208	-3.51	4.698
2,6 -DNT	-8.37	-3.78	4.59
1,2 -DNB	-8.019	-3.483	4.536
DAP-RGO	-5.292	-1.36	3.932

Table S3 : Different distances between interacting atoms in DFT optimized structure of TNP and DAP-RGO:

Type of interaction	Electrostatic interaction	Hydrogen bonding interaction		
Between atoms	**$O_{(106)}$ - $H_{(107)}$**	**$O_{(103)}$ - $H_{(96)}$**	**$O_{(100)}$ - $H_{(85)}$**	**$O_{(105)}$ - $H_{(84)}$**
Distance (Å)	1.82	1.99	1.92	2.05

Table S4 : Different distances between interacting atoms in DFT optimized structure of 2, 6-DNT and DAP-RGO:

Type of interaction	Hydrogen bonding interaction		
Between atoms	**$O_{(102)}$ - $H_{(184)}$**	**$O_{(100)}$ - $H_{(68)}$**	**$O_{(99)}$ - $H_{(85)}$**
Distance (Å)	2.146	2.149	2.441

References:

1. Dinda, D.; Gupta, A.; Saha, S. K. Removal of Toxic Cr(VI) by UV-Active Functionalized Graphene Oxide for Water Purification. *J. Mater. Chem. A*. **2013**, *1*, 11221-11228.
2. Gupta, A.; Shaw, B. K.; Saha, S. K. Bright Green Photoluminescence in Aminoazobenzene-Functionalized Graphene Oxide. *J. Phys. Chem. C*. **2014**, *118*, 6972−6979.
3. Melhuis, W. H. Quantum Efficiencies of Fluorescence of Organic Substances: Effect of Solvent and Concentration of the Fluorescent Solute. *J. Phys. Chem*. **1961**, *65*, 229–235.
4. Mei, Q.; Zhang, K.; Guan, G.; Liu, B.; Wang, S.; Zhang, Z. Highly Efficient Photoluminescent Graphene Oxide with Tunable Surface Properties. *Chem.Commun*. **2010**, *46*, 7319-7321.
5. Roy, B.; Bar, A. K.; Gole, B.; Mukherjee, P. S. Fluorescent Tris-Imidazolium Sensors for Picric Acid Explosive. *J. Org. Chem*. **2013**, *78*, 1306−1310.